Available online at website: https://journal.bcrec.id/index.php/bcrec

Bulletin of Chemical Reaction Engineering & Catalysis, 21 (2) 2026, 482-489

Original Research Article

Effect of Sodium Borohydride to Ferric Chloride Molar Ratios on Nanoscale Zero-Valent Iron for Hydrogen Generation from Formic Acid

Siti Aishah Yusuf[1], Meor Saiful Rizal Meor Ahmad Zubairi[2], Siti Fatimah Abdul Halim[1], Siu Hua Chang[1*]

[1]*Waste Management and Resources Recovery (WeResCue) Group, Faculty of Chemical Engineering, Universiti Teknologi MARA, Cawangan Pulau Pinang, 13500 Permatang Pauh, Pulau Pinang, Malaysia.*

[2]*Graphite Signature Sdn Bhd, 31650 Ipoh, Malaysia.*

Received: 13th January 2026; Revised: 4th March 2026; Accepted: 5th March 2026
Available online: 9th March 2026; Published regularly: August 2026

Abstract

Hydrogen generation from formic acid using nanoscale zero-valent iron (nZVI) represents a promising route for low-cost and sustainable hydrogen production. However, the effect of sodium borohydride ($NaBH_4$) to ferric chloride ($FeCl_3$) molar ratio on nZVI synthesis and performance remains insufficiently explored. This study investigated how varying $NaBH_4$:$FeCl_3$ molar ratios affect nZVI synthesis characteristics and its hydrogen generation efficiency from formic acid, which acts as a safe and easily handled hydrogen carrier. nZVI was synthesized through a one-step liquid-phase chemical reduction method using $NaBH_4$:$FeCl_3$ ratios ranging from 4.4:1 to 8.8:1. UV–Vis spectroscopy indicated that the 4.4:1 ratio yielded the highest nZVI formation, reflecting optimal reduction efficiency and particle formation. Hydrogen generation experiments conducted in a closed reactor equipped with a water displacement system revealed that nZVI synthesized at the 4.4:1 ratio achieved the maximum hydrogen volume (98 mL), which progressively declined to 53 mL at the 8.8:1 ratio. These findings demonstrate that precursor molar ratios significantly influence nZVI formation, stability, and reactivity toward hydrogen evolution. An optimal $NaBH_4$:$FeCl_3$ ratio of 4.4:1 was identified for maximizing nZVI formation and hydrogen volume, providing valuable insights for developing scalable formic acid–based hydrogen generation systems.

Keywords: Hydrogen; Nanoscale Zero-Valent Iron; Formic acid; Sodium borohydride; Molar Ratio

How to Cite: Yusuf, S. A., Meor Ahmad Zubairi, M. S. R., Abdul Halim, S. F., Chang, S. H. (2026). Effect of Sodium Borohydride to Ferric Chloride Molar Ratios on Nanoscale Zero-Valent Iron for Hydrogen Generation from Formic Acid. *Bulletin of Chemical Reaction Engineering & Catalysis*, 21 (2), 482-489. (DOI: 10.9767/bcrec.20634)

Permalink/DOI: https://doi.org/10.9767/bcrec.20634

1. Introduction

Hydrogen is a vital industrial commodity extensively used in ammonia synthesis, petroleum refining, methanol production, and the steel industry [1,2]. Global hydrogen demand exceeded 94 million tonnes in 2021 and continues to rise, driven by the growth of the industrial and energy sectors [3]. Currently, more than 99% of hydrogen is produced from fossil-based processes such as steam methane reforming, partial oxidation of hydrocarbons, and coal gasification [4]. These methods are energy-intensive and generate substantial greenhouse gas emissions. Although water electrolysis offers a cleaner option using renewable electricity, its widespread adoption remains constrained by high energy costs and dependency on intermittent renewable sources [5]. Therefore, developing simpler and more sustainable hydrogen production routes is urgently required, mirroring similar efforts being implemented across other industrial processes [6–8].

* Corresponding Author.
Email: shchang@uitm.edu.my (S. H. Chang)

Among emerging approaches, formic acid (HCOOH) has attracted attention as a liquid hydrogen carrier due to its high hydrogen content (4.4 wt%), safety, and stability under ambient conditions [9]. Conventional formic acid decomposition typically relies on noble metal catalysts such as palladium, platinum, and ruthenium [10]. However, these catalysts are expensive and may produce carbon-containing byproducts such as CO and CO_2, particularly when low-cost base metals are used [11]. Recently, Singh *et al.* [12] demonstrated that nZVI can generate hydrogen from formic acid through a direct redox process without forming carbon-containing gaseous byproducts, as expressed in Equation (1):

$$Fe^0_{(s)} + 2HCOOH_{(\ell)} + 2H_2O \rightarrow Fe(HCOO)_2.2H_2O_{(s)} + H_{2(g)} \quad (1)$$

In this system, hydrogen evolution proceeds through a direct redox mechanism rather than a catalytic pathway. Fe^0 acts as a sacrificial reductant and electron donor. Upon contact with formic acid, surface Fe^0 atoms are oxidized to Fe^{2+} [12].

$$Fe^0 \rightarrow Fe^{2+} + 2e^- \quad (2)$$

The released electrons are transferred to protons generated from the dissociation of formic acid in aqueous solution:

$$HCOOH \rightleftharpoons H^+ + HCOO^- \quad (3)$$
$$2H^+ + 2e^- \rightarrow H_2(g) \quad (4)$$

The overall simplified reaction can therefore be written as:

$$Fe^0 + 2HCOOH \rightarrow Fe^{2+} + 2HCOO^- + H_2(g) \quad (5)$$

The electron transfer and hydrogen generation process is illustrated in Figure 1. The electron transfer occurs directly at the nZVI surface, where adsorbed protons are reduced to molecular hydrogen. The nanoscale dimension of nZVI enhances this process by providing a high surface area, short electron diffusion pathways, and abundant active Fe^0 sites. Importantly, Fe^0 is consumed during the reaction, confirming its role as a stoichiometric reductant rather than a catalyst. The generated Fe^{2+} subsequently coordinates with formate ions to form stable iron(II) formate dihydrate, $Fe(HCOO)_2 \cdot 2H_2O$. This mechanism explains the high hydrogen purity and the absence of carbon-containing gaseous byproducts.

The nZVI can be synthesized through various methods, including ball milling, carbothermal reduction, ultrasound-assisted techniques, biological routes, and chemical reduction [13–19]. Among these, chemical reduction using sodium borohydride ($NaBH_4$) is the most widely adopted due to its simplicity and ability to produce high-purity nanoparticles. The synthesis typically follows the reaction shown in Equation (6) [20]:

$$2FeCl_3 + 6NaBH_4 + 18H_2O \rightarrow 2Fe^0 + 6NaCl + 6B(OH)_3 + 21H_2 \quad (6)$$

In this method, the $NaBH_4$:$FeCl_3$ molar ratio plays a critical role in determining reduction efficiency and particle characteristics. Although a theoretical ratio of 3:1 is required for complete reduction of Fe^{3+} to Fe^0, excess $NaBH_4$ is often used to compensate for hydrolysis and side reactions [13,21,22]. However, excessive $NaBH_4$

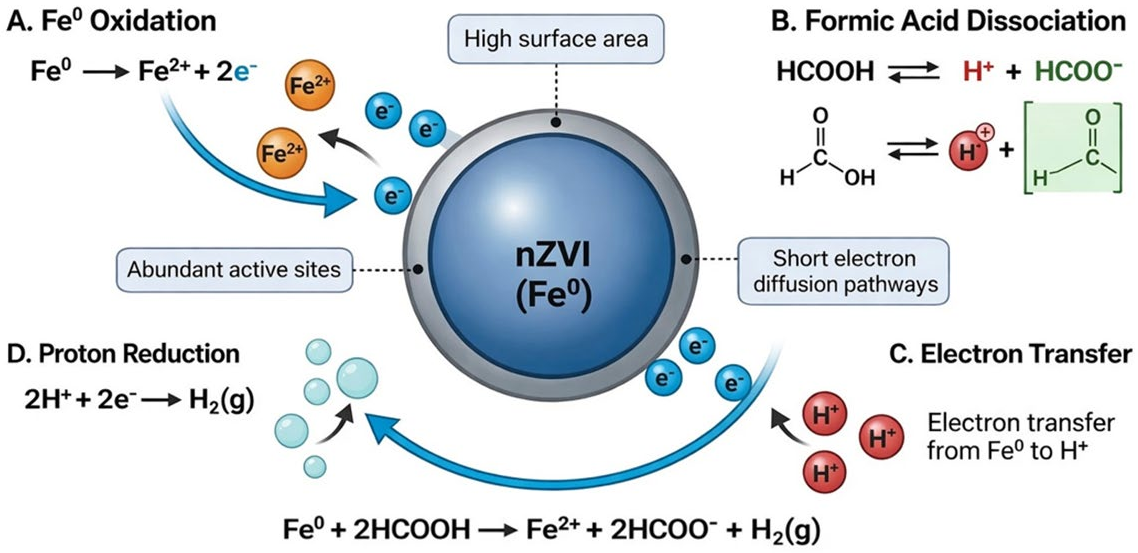

Figure 1. Mechanism of redox reaction.

may promote rapid hydrogen evolution, particle aggregation, and surface passivation [23–25]. Therefore, identifying an optimal $NaBH_4$:$FeCl_3$ molar ratio exceeding the theoretical stoichiometric requirement is essential for achieving efficient and controlled nZVI synthesis.

Despite the importance of this parameter, limited studies have systematically evaluated how variations in the $NaBH_4$:$FeCl_3$ molar ratio influence nZVI formation and its hydrogen generation performance during formic acid reduction. To address this gap, the present study investigated the effect of $NaBH_4$:$FeCl_3$ molar ratios ranging from 4.4:1 to 8.8:1 on nZVI synthesis and its hydrogen production efficiency. The results provide new insights into the relationship between synthesis conditions and nZVI performance, supporting the development of cost-effective and scalable hydrogen generation systems.

2. Materials and Methods

2.1 Materials

Iron(III) chloride hexahydrate ($FeCl_3.6H_2O$), ethanol (C_2H_5OH, 99.7% v/v), and formic acid (CH_2O_2, 90% v/v) were obtained from R&M Chemicals, while sodium borohydride ($NaBH_4$) was supplied by Bellamy Precision, Malaysia. All chemicals were used as received without any further purification or modification.

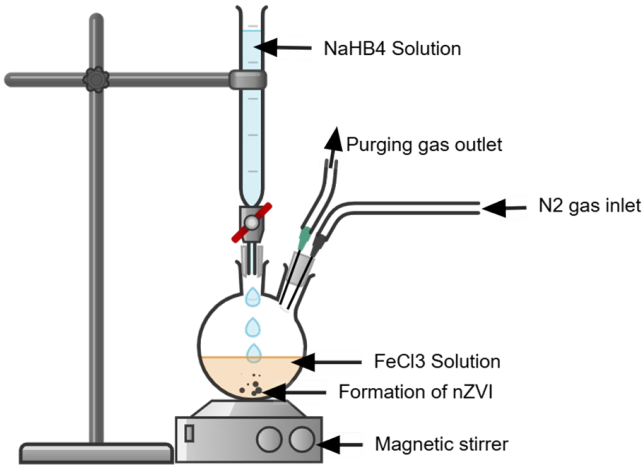

Figure 2. Experimental setup for nZVI synthesis.

2.2. Synthesis of nZVI

The nZVI was synthesized via the chemical reduction of $FeCl_3.6H_2O$ using $NaBH_4$ as the reductant at various $NaBH_4$:$FeCl_3$ molar ratios ranging from 4.4:1 to 8.8:1, following the procedure reported by Singh *et al.* [12]. The specific molarities and mass of $NaBH_4$ and $FeCl_3$ solutions used for each ratio are summarized in Table 1. $NaBH_4$ solutions were prepared by dissolving the required amount (g) of $NaBH_4$ powder in 55 mL of deionized water, while $FeCl_3$ solutions were prepared by dissolving a known mass of $FeCl_3 \cdot 6H_2O$ in 12.5 mL of an ethanol-to-water mixture (4:1 v/v) [24].

Figure 2 shows the experimental setup used for nZVI synthesis. Prior to synthesis, the entire experimental setup was purged with nitrogen gas at a flow rate of 50 mL/min for 15 minutes to remove dissolved oxygen and establish an inert atmosphere, thereby preventing premature oxidation of Fe^{2+}/Fe^{3+} species and freshly formed nZVI. The $NaBH_4$ solution was then added dropwise to the $FeCl_3$ solution under vigorous stirring at room temperature (600 rpm), while maintaining a continuous nitrogen flow. The appearance of a black precipitate indicated the formation of nZVI [24]. After 10 minutes of reaction, the precipitated nanoparticles were collected by centrifugation and washed thoroughly with ethanol to remove residual ions and byproducts [26]. The purified nZVI was then stored as suspension in ethanol to prevent oxidation [18]. Each nZVI suspension was subsequently freeze-dried to obtain a dry powder prior to use in hydrogen generation experiments.

2.3. Hydrogen Generation Experiments

Hydrogen generation experiments were conducted in a closed, three-neck round-bottom flask serving as the reaction vessel, as illustrated in Figure 3. The central neck was fitted with a rubber septum for the introduction of nZVI powder and injection of formic acid (50% v/v) via syringe. One of the side necks was connected through rubber tubing to an inverted, water-filled burette for hydrogen gas collection by water displacement, while the other side neck was connected to a nitrogen gas line to establish an

Table 1. Molarities of $NaBH_4$ and $FeCl_3$ solutions used at different $NaBH_4$:$FeCl_3$ molar ratios.

Molar ratio		Number of moles		Molarity (mol/L)		Mass (g)	
$NaBH_4$	$FeCl_3$	$NaBH_4$	$FeCl_3$	$NaBH_4$	$FeCl_3$	$NaBH_4$	$FeCl_3$
4.4	1	0.01320	0.00300	0.24000	0.24000	0.49936	0.81090
5.5	1	0.01320	0.00240	0.24000	0.19200	0.49936	0.64872
6.6	1	0.01320	0.00200	0.24000	0.16000	0.49936	0.54060
7.7	1	0.01320	0.00171	0.24000	0.13710	0.49936	0.46337
8.8	1	0.01320	0.00150	0.24000	0.12000	0.49936	0.40545

inert atmosphere within the reactor. Prior to each experiment, the reaction vessel was purged with high purity nitrogen gas (99.99%) at a flow rate of 50 mL.min^{-1} for 15 minutes to remove dissolved oxygen and establish an inert atmosphere. After purging, the nitrogen line was sealed with a clamp to preserve the inert environment throughout the reaction. The gas collection system was allowed to stabilize until the burette water level remained constant, and no gas displacement was observed before the initiation of the reaction. Gas evolution commenced only upon contact between nZVI and formic acid, indicating that the collected gas originated exclusively from the reaction. Therefore, contamination from external nitrogen or atmospheric gases was considered negligible. The use of a sealed reactor configuration minimized gas leakage and ensured accurate quantification of the evolved hydrogen. All tubing, joints, and seals were inspected prior to each run to maintain airtight operation.

Hydrogen generation was first tested using nZVI synthesized at a $NaBH_4$:$FeCl_3$ molar ratio of 4.4:1, followed by experiments employing ratios of 5.5:1, 6.6:1, 7.7:1, and 8.8:1 to assess the effect of synthesis ratio on hydrogen volume. In each run, 0.25 g of nZVI powder was introduced into the reactor, followed by the injection of 10 mL of 50% v/v formic acid. The reaction initiated immediately upon contact between nZVI and formic acid. All experiments were conducted at room temperature (25 ˚C) and maintained for 30 minutes. Each test was performed in triplicate, and the relative standard deviation of hydrogen volume among replicates was less than 5%. The composition of the evolved gas was then verified using Gas Chromatography equipped with Thermal Conductivity Detector (GC–TCD) analysis with nitrogen gas as a carrier gas to ascertain the hydrogen concentration in the gas mixture.

3. Results and Discussion

3.1. Effect of $NaBH_4$:$FeCl_3$ Molar Ratio on nZVI Formation

UV–Vis spectroscopy was employed to assess the formation of nZVI synthesized at varying $NaBH_4$:$FeCl_3$ molar ratios (4.4:1, 5.5:1, 6.6:1, 7.7:1, and 8.8:1). NZVI suspensions typically exhibit a broad absorption band between 250 and 320 nm, attributed to Fe^{2+}/Fe^{3+} transitions and charge-transfer processes, which indicates successful nanoparticle formation [18,27]. As shown in Figure 4, all samples displayed absorption within this region, confirming nZVI synthesis. However, clear differences in

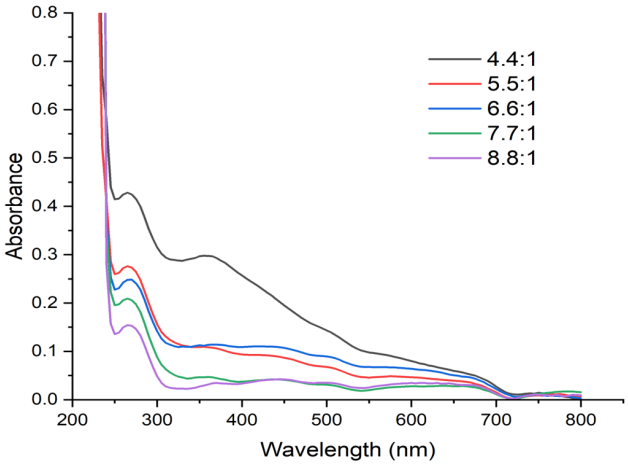

Figure 4. UV–Vis absorption spectra of nZVI synthesized at varying $NaBH_4$:$FeCl_3$ molar ratios (4.4:1, 5.5:1, 6.6:1, 7.7:1, and 8.8:1).

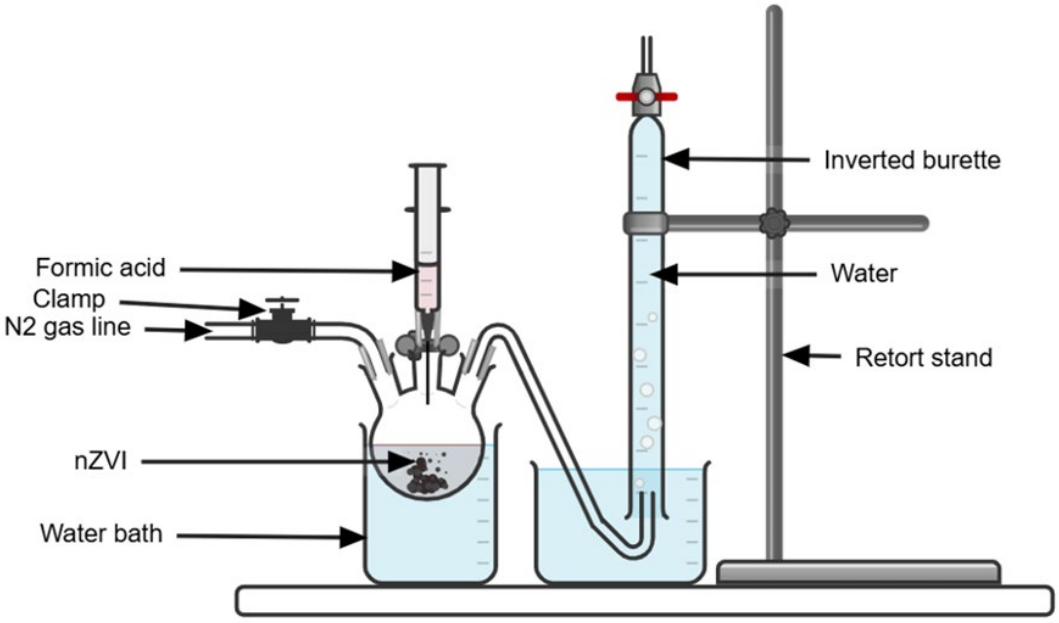

Figure 3. Experimental setup for hydrogen generation from formic acid using nZVI.

absorbance intensity were observed among the samples, indicating variations in nZVI yield.

The 4.4:1 $NaBH_4$:$FeCl_3$ ratio produced the most intense and well-defined absorption peak, indicating the highest nZVI yield. Increasing the $NaBH_4$ proportion resulted in a progressive decline in absorbance intensity, indicating lower nZVI formation efficiency at higher reductant concentrations. This reduction is likely due to the formation of boron-rich byproducts or borates that inhibit the complete reduction of Fe^{3+} ions and interfere with nanoparticle formation [25]. Excess $NaBH_4$ can also promote rapid nucleation and uncontrolled particle growth, leading to aggregation and surface passivation [10,12,19,28–30]. At higher molar ratios (≥7.7:1), broader and weaker absorption peaks were observed. These features suggest a more heterogeneous particle distribution and increased surface oxidation, both of which reduce spectral intensity and definition.

Previous studies have reported similar trends. Song *et al.* [21], found that lower $NaBH_4$ concentrations produced more reactive nZVI for trichloroethylene reduction, while Yuvakkumar *et al.* [18] and Hwang *et al.* [22] observed that excessive reductant concentrations enhanced nucleation but decreased stability. Turabik *et al.* [23] further demonstrated that both insufficient and excessive $NaBH_4$ lead to poorly stabilized nZVI. These findings highlight the importance of a balanced molar ratio. Overall, the results indicate that the 4.4:1 ratio yields the highest-quality nZVI with improved stability, while higher ratios promote aggregation and surface passivation. This inverse relationship between $NaBH_4$ concentration and nZVI yield underscores the need to optimize synthesis conditions for efficient hydrogen generation.

3.2 Effect of $NaBH_4$:$FeCl_3$ Molar Ratio on Hydrogen Generation

Figure 5 shows the hydrogen volume generated from formic acid reduction using 25 g/L of nZVI synthesized at $NaBH_4$:$FeCl_3$ molar ratios

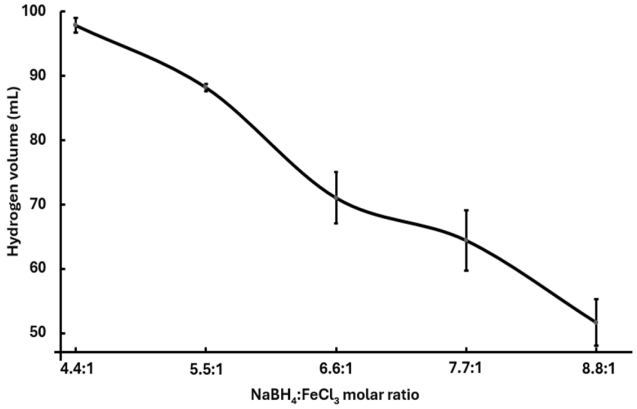

Figure 5. Effect of $NaBH_4$:$FeCl_3$ molar ratio on hydrogen volume in 50% v/v formic acid over 30 min reaction time.

of 4.4:1–8.8:1 after 30 minutes at room temperature with 50% (v/v) formic acid, with the relative standard deviation of hydrogen volume among replicates was less than 5%. A clear decreasing trend in hydrogen volume was observed as the $NaBH_4$:$FeCl_3$ ratio increased. The highest hydrogen volume (98 mL) was achieved at the 4.4:1 ratio. In contrast, only 53 mL was produced at the 8.8:1 ratio. This significant decline suggests that excessive $NaBH_4$ adversely affects nZVI reactivity. The reduced hydrogen generation at higher molar ratios may be attributed to several factors, including boron-rich byproduct formation, nanoparticle aggregation, and surface passivation, which collectively decrease the redox activity of nZVI [21,23]. This decline is consistent with the UV–Vis results discussed in Section 3.1, indicating that excess $NaBH_4$ reduces the formation of reactive nZVI for hydrogen generation. While previous studies (e.g., Song *et al.* [21], Yuvakkumar *et al.* [18], Hwang *et al.* [22] and Turabik *et al.* [23]) explored nZVI synthesis and particle behavior under various reducing conditions, they did not systematically evaluated the combined influence of reductant-to-precursor molar ratios on hydrogen generation performance. In contrast, the present study directly correlates synthesis molar ratios with hydrogen evolution efficiency, thereby addressing this key research gap as shown in Table 2.

Overall, these findings demonstrate that maintaining a 4.4:1 $NaBH_4$:$FeCl_3$ ratio is essential not only for optimizing nanoparticle formation but also for maximizing hydrogen volume. Unlike previous reports, this study provides a systematic assessment of how synthesis molar ratios govern nZVI reactivity in formic acid reduction. Future studies should focus on kinetic modeling, mechanistic analysis of nZVI–formate interactions, and the incorporation of stabilizing support materials to minimize aggregation and enhance the reusability of nZVI, similar to other nanomaterial-based systems [33,34]. Evaluating nZVI performance in continuous or pilot-scale systems is also recommended to advance its application in sustainable hydrogen production technologies.

3.3 Hydrogen Purity and Gas Composition

The evolved gas mixture was characterised by GC-TCD to determine hydrogen purity and quantify the composition of gaseous products generated from the nZVI by formic acid reduction. Table 3 shows the concentrations of the gaseous species detected in the collected samples. As summarised in Table 3, hydrogen accounted for 99.81 mol% of the total detected gas, indicating that the nZVI predominantly produces hydrogen with negligible interference from other gaseous species. Only trace amounts

of CO_2 (0.14 mol%) and CO (0.05 mol%) were detected, confirming minimal side reactions following correction for the blank response. This level of hydrogen purity is consistent with prior results from nZVI-based hydrogen production systems. For instance, hydrogen produced from a nZVI dissolution system was reported to contain minimal levels of common gaseous impurities such as CO_2 and CH_4, indicating that nZVI itself can serve as a direct source of hydrogen in biomass-based systems [35]. Compared to previous findings, the present system has a high hydrogen purity, showing that the nZVI can produce high-purity hydrogen with little gaseous byproducts, highlighting their potential for clean and sustainable energy applications.

4. Conclusions

This study systematically investigated the effect of $NaBH_4$:$FeCl_3$ molar ratios on the synthesis of nZVI and its performance in hydrogen generation via formic acid reduction. UV–Vis spectroscopy revealed that the $NaBH_4$:$FeCl_3$ molar ratio significantly influenced nZVI formation, with the 4.4:1 ratio producing the highest absorbance intensity and thus the most effective nZVI formation. Increasing the $NaBH_4$ proportion led to a gradual decline in absorbance, likely due to the formation of excess boron-rich by-products that promoted particle agglomeration and surface passivation, thereby reducing the amount of reactive nZVI formed. These effects were consistent with the hydrogen generation results, where nZVI synthesized at the 4.4:1 ratio

Table 2. Comparison table of relevant literature alongside the present study.

No.	Material characteristics	Reaction conditions	Hydrogen generation performance	Molar ratio study	Ref.
1.	nZV+-formic acid	Formic acid reduction, closed reactor with water displacement system	Max H_2: 98 mL at 4.4:1; decreases to 53 mL at 8.8:1	Yes; optimal $NaBH_4$:$FeCl_3$ ratio 4.4:1 enhances nZVI formation and H_2 generation	This study
2.	nZVI+formic acid	0.1 g uncoated ferrobots in 2 mL aqueous FA (10–100%), gas collected after 1 min	H_2 volume increases with FA concentration (max ~0.75 mL at 50–60 vol%) and ferrobot mass; rate highest at ~2 min reaction time	Not studied	[12]
3.	nZVI+formic acid	Formic acid decomposition, varying nZVI dosage (200–1000 g/L), temperature (25–75°C), reaction time (5–30 min)	Max H_2: 215 mL at 800 g/L nZVI, 25°C, 30 min; surface area decrease after reaction correlates with lower H_2 volume	Not studied	[24]
4.	nZVI+weak acid	Microsize Fe^0 or scrap iron with $NaHCO_3$ and citric acid under mild anaerobic conditions	H_2 production rate: 0.09–0.55 g(H_2)/kg(Fe^0)·h; >85 vol% H_2 after 1 day and >94 vol% H_2 at end of each cycle; negligible H_2 without bicarbonate	Not studied	[31]
5.	nZVI + Ascorbic acid	Photo fermentation of bean dregs and corn stover, initial pH 9	Max H_2: 767.5 ± 2.8 mL	Not studied	[32]
6.	nZVI	Synthesis of ZVI particles with varying Fe^{3+}, $NaBH_4$, stabilizer, temperature, pH, and stirring rates	Not studied	Yes; particle size influenced by synthesis parameters	[23]

Table 3. Concentration of gases collected from formic acid reduction with nZVI.

Total gas concentration (% mole)	Gas concentration (% mole)		
	H_2	CO_2	CO
49.17	99.81	0.14	0.05

yielded the highest hydrogen volume (98 mL). Higher $NaBH_4$:$FeCl_3$ ratios significantly reduced hydrogen output, confirming that precursor molar ratios critically determine the redox activity and reactivity of nZVI in the formic acid reduction pathway. Overall, maintaining a 4.4:1 $NaBH_4$:$FeCl_3$ ratio was found to be optimal for balancing nanoparticle formation, stability, and hydrogen volume. These findings provide valuable insights for designing cost-effective and scalable formic acid-based hydrogen production systems using nZVI.

Acknowledgment

The authors gratefully acknowledge the Ministry of Higher Education (MOHE), Malaysia, for financial support through the Fundamental Research Grant Scheme (FRGS/1/2022/TK08/UITM/02/5 and FRGS/1/2023/TK08/UITM/02/10) and Universiti Teknologi MARA (UiTM) via the UiTM Conference Support Fund. Special thanks to Universiti Sains Malaysia (USM), Nibong Tebal, for access to key instruments.

CRedit Author Statement

Author Contributions: S.A Yusuf: Conceptualization, Methodology, Investigation, Writing Original Draft, Writing, Review and Editing, Visualization; M.S.R.M.A. Zubair: Resources, Supervision ; S.F.A. Halim: Supervision, Funding acquisition ; S.H. Chang: Conceptualization, Validation, Writing, Review and Editing, Supervision, Funding acquisition. All authors have read and agreed to the published version of the manuscript.

References

[1] Ramachandran, R., Menon, R.K. (1998). An overview of industrial uses of hydrogen. *Int. J. Hydrogen Energy*, 23, 593–598. DOI: 10.1016/s0360-3199(97)00112-2

[2] Liu, W., Zuo, H., Wang, J., Xue, Q., Ren, B., Yang, F. (2021). The production and application of hydrogen in steel industry. *Int. J. Hydrogen Energy*, 46, 10548–10569. DOI: 10.1016/j.ijhydene.2020.12.123

[3] Mozakka, M., Salimi, M., Hosseinpour, M. (2024). Determining the challenges of transition to a hydrogen economy through developing a quantitative index. *International Journal of Hydrogen Energy*, 56, 1301–1308. DOI: 10.1016/j.ijhydene.2023.12.297.

[4] Gunawardane, K. (2023). Evolution of hydrogen energy and its potential opportunities around the globe. In: *Hydrogen Energy Conversion and Management*. Elsevier, pp. 3–33. DOI: 10.1016/B978-0-443-15329-7.00007-7.

[5] Chang, S.H., Rajuli, M.F. (2024). An overview of pure hydrogen production via electrolysis and hydrolysis. *Int. J. Hydrogen Energy*, 84, 521–538. DOI: 10.1016/j.ijhydene.2024.08.245

[6] Chang, S.H. (2017). Parametric studies on an innovative waste vegetable oil-based continuous liquid membrane (WVCLM) for Cu(II) ion separation from aqueous solutions. *Journal of Industrial and Engineering Chemistry*, 50, 102–110. DOI: 10.1016/j.jiec.2017.01.037.

[7] Chang, S.H., Jampang, A.O.A. (2021). Green extraction of gold(III) and copper(II) from chloride media by palm kernel fatty acid distillate. *Journal of Water Process Engineering*, 43. DOI: 10.1016/j.jwpe.2021.102298.

[8] Halim, S.F.A., Chang, S.H., Morad, N. (2020). Extraction of Cu(II) ions from aqueous solutions by free fatty acid-rich oils as green extractants. *Journal of Water Process Engineering*, 33. DOI: 10.1016/j.jwpe.2019.100997.

[9] Eppinger, J., Huang, K.W. (2017). Formic Acid as a Hydrogen Energy Carrier. *ACS Energy Lett.*, 2, 188–195. DOI: 10.1021/acsenergylett.6b00574

[10] Wang, X., Meng, Q., Gao, L., Jin, Z., Ge, J., Liu, C., Xing, W. (2018). Recent progress in hydrogen production from formic acid decomposition. *Int. J. Hydrogen Energy*, 43, 7055–7071. DOI: 10.1016/j.ijhydene.2018.02.146

[11] Singh, A.K., Singh, S., Kumar, A. (2016). Hydrogen energy future with formic acid: A renewable chemical hydrogen storage system. *Catal. Sci. Technol.* 6, 12–40. DOI: 10.1039/c5cy01276g

[12] Singh, A.K., Rarotra, S., Pasumarthi, V., Mandal, T.K., Bandyopadhyay, D. (2018). Formic acid powered reusable autonomous ferrobots for efficient hydrogen generation under ambient conditions. *Journal of Materials Chemistry A*, 6(19), 9209–9219. DOI: 10.1039/c8ta02205d.

[13] Jamei, M.R., Khosravi, M.R., Anvaripour, B. (2014). A novel ultrasound assisted method in synthesis of NZVI particles. *Ultrasonics Sonochemistry*, 21(1), 226–233. DOI: 10.1016/j.ultsonch.2013.04.015.

[14] Zhang, Y., Tang, Y., Yan, R., Liang, S., Liu, Z., Yang, Y. (2024). Green-synthesized, biochar-supported nZVI from mango kernel residue for aqueous hexavalent chromium removal: Performance, mechanism and regeneration. *Chinese Journal of Chemical Engineering*, 71, 91–101. DOI: 10.1016/j.cjche.2024.04.009.

[15] Sathish, T., Masih, J., Gupta, A., Kumar, A., Raja, L., Singh, V., Al-Enizi, A.M., Pandit, B., Gupta, M., Senthilkumar, N., Yusuf, M. (2024). Sustainable nanoparticles of Non-Zero-valent iron (nZVI) production from various biological wastes. *Journal of King Saud University - Science*, 36(11), 103553. DOI: 10.1016/j.jksus.2024.103553.

[16] Bounab, N., Duclaux, L., Reinert, L., Oumedjbeur, A., Boukhalfa, C., Penhoud, P., Muller, F. (2021). Improvement of zero valent iron nanoparticles by ultrasound-assisted synthesis, study of Cr(VI) removal and application for the treatment of metal surface processing wastewater. *Journal of Environmental Chemical Engineering*, 9(1), 104773. DOI: 10.1016/j.jece.2020.104773.

[17] Pandey, K., Sharma, S., Saha, S. (2022). Advances in design and synthesis of stabilized zero-valent iron nanoparticles for groundwater remediation. *Journal of Environmental Chemical Engineering*, 10(3), 107993. DOI: 10.1016/j.jece.2022.107993.

[18] Yuvakkumar, R., Elango, V., Rajendran, V., Kannan, N. (2011). Preparation and characterization of zero valent Iron nanoparticles. *Digest Journal of Nanomaterials and Biostructures*, 6(4), 1771–1776.

[19] Pasinszki, T., Krebsz, M. (2020). Synthesis and application of zero-valent iron nanoparticles in water treatment, environmental remediation, catalysis, and their biological effects. *Nanomaterials*, 10. DOI: 10.3390/nano10050917

[20] Boonruam, P., Soisuwan, S., Wattanachai, P., Morillas, H., Upasen, S. (2020). Solvent effect on zero-valent iron nanoparticles (nZVI) preparation and its thermal oxidation characteristic. *ASEAN Engineering Journal*, 10(2), 1–12. DOI: 10.11113/aej.v10.16525.

[21] Song, H.-C., Carraway, E.R., Kim, Y.-H. (2005). Synthesis of Nano-Sized Iron for Reductive Dechlorination. 2. Effects of Synthesis Conditions on Iron Reactivities. *Environmental Engineering Research*, 10(4), 174–180. DOI: 10.4491/eer.2005.10.4.174.

[22] Hwang, Y.H., Kim, D.G., Shin, H.S. (2011). Effects of synthesis conditions on the characteristics and reactivity of nano scale zero valent iron. *Applied Catalysis B: Environmental*, 105 (1–2), 144–150. DOI: 10.1016/j.apcatb.2011.04.005.

[23] Turabik, M., Simsek, U.B. (2017). Effect of synthesis parameters on the particle size of the zero valent iron particles. *Inorganic and Nano-Metal Chemistry*, 47(7), 1033–1043. DOI: 10.1080/15533174.2016.1219869.

[24] Yusuf, S.A., Ismail, S.N.S., Zubairi, M.S.R.M.A., Muthuraman, G., Halim, S.F.A., Chang, S.H. (2025). Hydrogen Production by Formic Acid Decomposition with Nanoscale Zero-Valent Iron (nZVI): Effects of nZVI Dosage, Temperature and Time. *Journal of Advanced Research in Fluid Mechanics and Thermal Sciences*, 125(1), 158–166. DOI: 10.37934/arfmts.125.1.158166.

[25] Bae, S., Collins, R.N., Waite, T.D., Hanna, K. (2018). Advances in Surface Passivation of Nanoscale Zerovalent Iron: A Critical Review. *Environmental Science and Technology*, 52(21), 12010–12025. DOI: 10.1021/acs.est.8b01734.

[26] Visentin, C., Trentin, A.W. da S., Braun, A.B., Thomé, A. (2021). Nano scale zero valent iron production methods applied to contaminated sites remediation: An overview of production and environmental aspects. *J. Hazard. Mater*. 410, 124614. DOI: 10.1016/j.jhazmat.2020.124614

[27] Rahman, N., Nasir, M., Bharti, M., Samdani, M.S. (2023). Fabrication of Zero-Valent Iron Nanoparticles Impregnated Cross-Linked Chitosan Grafted ß-Cyclodextrin for Removal of Cloxacillin from Aqueous Environment. *Journal of Inorganic and Organometallic Polymers and Materials*, 34(4), 1654–1677. DOI: 10.1007/s10904-023-02907-2.

[28] Tang, H., Wang, J., Zhang, S., Pang, H., Wang, X., Chen, Z., Li, M., Song, G., Qiu, M., Yu, S. (2021). Recent advances in nanoscale zero-valent iron-based materials: Characteristics, environmental remediation and challenges. *J. Clean. Prod.* 319, 128641. DOI: 10.1016/j.jclepro.2021.128641

[29] Chen, K.F., Li, S., Zhang, W.X. (2011). Renewable hydrogen generation by bimetallic zero valent iron nanoparticles. *Chemical Engineering Journal*, 170(2–3), 562–567. DOI: 10.1016/j.cej.2010.12.019.

[30] Shamsuri, S.R.S., Saifudin, K.N., Othman, I.S., Ismail, S., Rashid, M.W.A., Moriga, T. (2024). Synthesis of Ni Nanoparticle with Controlled Morphology via Liquid Phase Reduction Method. *Journal of Advanced Research in Micro and Nano Engineering*, 24(1), 46–51. DOI: 10.37934/ARMNE.24.1.4651.

[31] Gao, Y., Gao, X., Zhang, X. (2023). Hydrogen generation by soluble CO2 reaction with zero-valent iron or scrap iron and the role of weak acids for controlling FeCO3 formation. *Sustainable Energy Technologies and Assessments*, 56(2), 103061. DOI: 10.1016/J.ENG.2017.01.022.

[32] Zhu, S., Zhang, Y., Zhang, Z., Ai, F., Zhang, H., Li, Y., Wang, Y., Zhang, Q. (2023). Ascorbic acid-mediated zero-valent iron enhanced hydrogen production potential of bean dregs and corn stover by photo fermentation. *Bioresource Technology*, 374, 128761. DOI: 10.1016/j.biortech.2023.128761.

[33] Chang, S.H., Jampang, A.O.A., Din, A.T.M. (2025). Adsorption isotherms, kinetics, and thermodynamics of Au(III) on chitosan/palm kernel fatty acid distillate/magnetite nanocomposites. *International Journal of Biological Macromolecules*, 304. DOI: 10.1016/j.ijbiomac.2025.140913.

[34] Chang, S.H., Jampang, A.O.A. (2023). Enhanced adsorption selectivity of Au(III) over Cu(II) from acidic chloride solutions by chitosan/palm kernel fatty acid distillate/magnetite nanocomposites. *International Journal of Biological Macromolecules*, 252. DOI: 10.1016/j.ijbiomac.2023.126491.

[35] Huang, Y.X., Guo, J., Zhang, C., Hu, Z. (2016). Hydrogen production from the dissolution of nano zero valent iron and its effect on anaerobic digestion. *Water Research*, 88(2), 475–480. DOI: 10.1016/j.watres.2015.10.028.